

Scatter-plate microscopy with spatially coherent illumination and temporal scatter modulation: supplement

STEPHAN LUDWIG,^{1,*} PAVEL RUCHKA,¹ GIANCARLO PEDRINI,¹  XIANG PENG,² AND WOLFGANG OSTEN¹

¹University Stuttgart, Institut für Technische Optik, Stuttgart, 70569, Germany

²College of Physics and Optoelectronic Engineering, Key Laboratory of Optoelectronic Devices and Systems of Ministry of Education and Guangdong Province, Shenzhen University, Shenzhen, 518060, China

*ludwig@ito.uni-stuttgart.de

This supplement published with The Optical Society on 28 January 2021 by The Authors under the terms of the [Creative Commons Attribution 4.0 License](https://creativecommons.org/licenses/by/4.0/) in the format provided by the authors and unedited. Further distribution of this work must maintain attribution to the author(s) and the published article's title, journal citation, and DOI.

Supplement DOI: <https://doi.org/10.6084/m9.figshare.13437653>

Parent Article DOI: <https://doi.org/10.1364/OE.412047>

Scatter-plate microscopy with spatially coherent illumination and temporal scatter modulation: supplemental document

In scatter-plate microscopy (SPM), a speckle size larger than the pixel size of the sensor is essential. Here we want to discuss how the speckle size depends on the parameters of the setup.

1. THE SPECKLE SIZE IN SPM

A. Definition of the speckle size

The mean speckle radius Δr can be defined as the range over which the normalized covariance function of the speckle intensity falls below the value of e^{-1} , with e being the Euler's number. For paraxial field propagation (small scattering angles) and a sufficiently small correlation extent in the wave field the normalized covariance function of the speckle intensity $c_I(x, y)$ is given by [1]

$$c_I(x, y) = \left| \frac{\int \int_{-\infty}^{\infty} I(\alpha, \beta) \exp\left(-i \frac{2\pi}{\lambda z_2} (\chi x + \eta y)\right) d\chi d\eta}{\int \int_{-\infty}^{\infty} I(\chi, \eta) d\chi d\eta} \right|^2, \quad (\text{S1})$$

with λ the wavelength, z_2 the distance between the scattering surface and the recording sensor, $I(\chi, \eta)$ the intensity distribution illuminating the scattering surface, χ and η the coordinates in the scattering plane and x and y the coordinates in the recording plane.

For a circular symmetric intensity distributions ($I(\chi, \eta) = I(\rho)$ and consequently $c_I(x, y) = c_I(r)$. ρ and r are radial coordinates in the scatter and in the sensor plane, respectively) Eq. (S1) can be simplified [2]:

$$c_I(r) = \left| \frac{\int_0^{\infty} \rho I(\rho) J_0\left(\frac{2\pi r}{\lambda z_2} \rho\right) d\rho}{\int_0^{\infty} \rho I(\rho) d\rho} \right|^2, \quad (\text{S2})$$

with J_0 the Bessel function of the first kind, order zero.

B. Speckle size for plane wave illumination

For a circular uniform intensity distribution of diameter D (plane wave illumination of a scattering surface limited by a circular aperture $I(\rho) = I_0$ for $\rho < D/2$) we can find an analytical solution of Eq. (S2) [1]:

$$c_I^{(PW)}(r) = \left| \frac{\int_0^{D/2} \rho J_0\left(\frac{2\pi r}{\lambda z_2} \rho\right) d\rho}{\int_0^{D/2} \rho I_0 d\rho} \right|^2 = \left| 2 \frac{J_1\left(\frac{\pi D r}{\lambda z_2}\right)}{\frac{\pi D r}{\lambda z_2}} \right|^2, \quad (\text{S3})$$

with J_1 being the Bessel function of first kind, order one. With Eq. (S3) we obtain for plane wave illumination

$$\Delta r_{PW} = 0.61 \frac{\lambda z_2}{D} \quad (\text{S4})$$

C. Speckle size for spherical wave illumination

However, in SPM the speckles are not generated by plane waves but by spherical waves illuminating a scatter-plate surface limited by a circular aperture of diameter D ($I(\rho) = I_0 / (\rho^2 + z_1^2)$, with z_1 the distance between the source of the spherical wave and the scatter plane). If the source of the spherical wave is located on the optical axis, the autocorrelation of the speckle pattern is consequently given by

$$c_I^{(SW)}(r) = \left| \frac{\int_0^{D/2} \rho \frac{1}{z_1^2 + \rho^2} J_0\left(\frac{2\pi r}{\lambda z_2} \rho\right) d\rho}{\int_0^{D/2} \rho \frac{1}{z_1^2 + \rho^2} d\rho} \right|^2 = \left| \frac{2 \int_0^{D/(2z_1)} \frac{y}{1+y^2} J_0\left(\frac{2\pi r z_1}{\lambda z_2} y\right) dy}{\ln\left[\left(\frac{D}{2z_1}\right)^2 + 1\right]} \right|^2. \quad (\text{S5})$$

In the paraxial regime the numerical aperture (NA) of the system is given by $NA = \frac{D}{2z_1}$. With the magnification of the SPM, $M = \frac{z_2}{z_1}$, we can write Eq. (S5) as:

$$c_I^{(SW)}(r) = \left| \frac{2 \int_0^{NA} \frac{y}{1+y^2} J_0\left(\frac{2\pi r}{\lambda M} y\right) dy}{\ln[NA^2 + 1]} \right|^2. \quad (\text{S6})$$

The magnification M and the NA determine the shape of the covariance peak and consequently the speckle size. Unfortunately there is no analytical solution of Eq. (S5) respectively Eq. (S6). However, for small NA we can use the approximation $\frac{y}{1+y^2} \approx y$ and obtain

$$c_I^{(PW)} \approx \left| \frac{D \lambda z_2 J_1\left(\frac{\pi D r}{\lambda z_2}\right)}{2\pi z_1^2 r \ln\left[\left(\frac{D}{2z_1}\right)^2 + 1\right]} \right|^2. \quad (\text{S7})$$

The implicit function

$$\left| \frac{D J_1\left(\frac{\pi D \Delta r_{SW}}{\lambda z_2}\right)}{2\pi z_1^2 \frac{\Delta r_{SW}}{\lambda z_2} \ln\left[\left(\frac{D}{2z_1}\right)^2 + 1\right]} \right|^2 = e^{-1} \quad (\text{S8})$$

gives the speckle radius Δr_{SW} depending on z_1 , z_2 , D and λ . Since the equation can also be solved for $\frac{\Delta r_{SW}}{\lambda z_2}$, the proportionality $\Delta r \propto \lambda z_2$ applies not only for plane wave but also for spherical wave illumination.

D. Validation

In Fig. S1 we compared the speckle sizes retrieved with Eq. (S8) with speckle sizes obtained by numerically evaluating Eq. (S5) for 5000 equal spaced r -values between 0 and 100 μm . For numerical integration, we used the composite trapezoidal rule with 50 equal sized subintervals per millimetre of D . Fig. S1 a) and d) demonstrate the proportionalities $\Delta r_{SW} \propto z_2$ respectively $\Delta r_{SW} \propto \lambda$. Fig. S1 b) and c) show that Δr_{SW} increases with shorter distances z_1 respectively with smaller diameters of the illuminated area. Further, we see in b) that for a fixed diameter D the speckle size decreases when z_1 increases, but since for very large z_1 the spherical illumination can be approximated by a plane wave illumination, there is a minimum speckle size. e)-h) demonstrate how the NA and the magnification M determine the speckle size. We used the correct value $NA = \sin(\alpha) = \frac{D}{\sqrt{D^2 + 4z_1^2}}$ and not the small angle approximation $\frac{D}{2z_1}$. In g) we can see that the speckle size is almost proportional to the magnification. In e) and f), the speckle sizes retrieved with Eq. (S8) are represented by the unfilled circles and the speckle sizes retrieved by numerical integration are represented by dots. In the other plots, dashed red lines represent the speckle sizes retrieved with Eq. (S8). As expected, for large NA (small z_1 , see Fig. S1 b) there is a discrepancy between the speckle size obtained with Eq. (S8) and the numerically determined speckle sizes.

REFERENCES

1. J. W. Goodman, ed., *Speckle phenomena in optics: theory and applications* (Roberts, Englewood, Colo, 2007).
2. J. W. Goodman, *Introduction to Fourier optics* (W.H. Freeman, Macmillan Learning, New York, 2017), fourth edition ed.

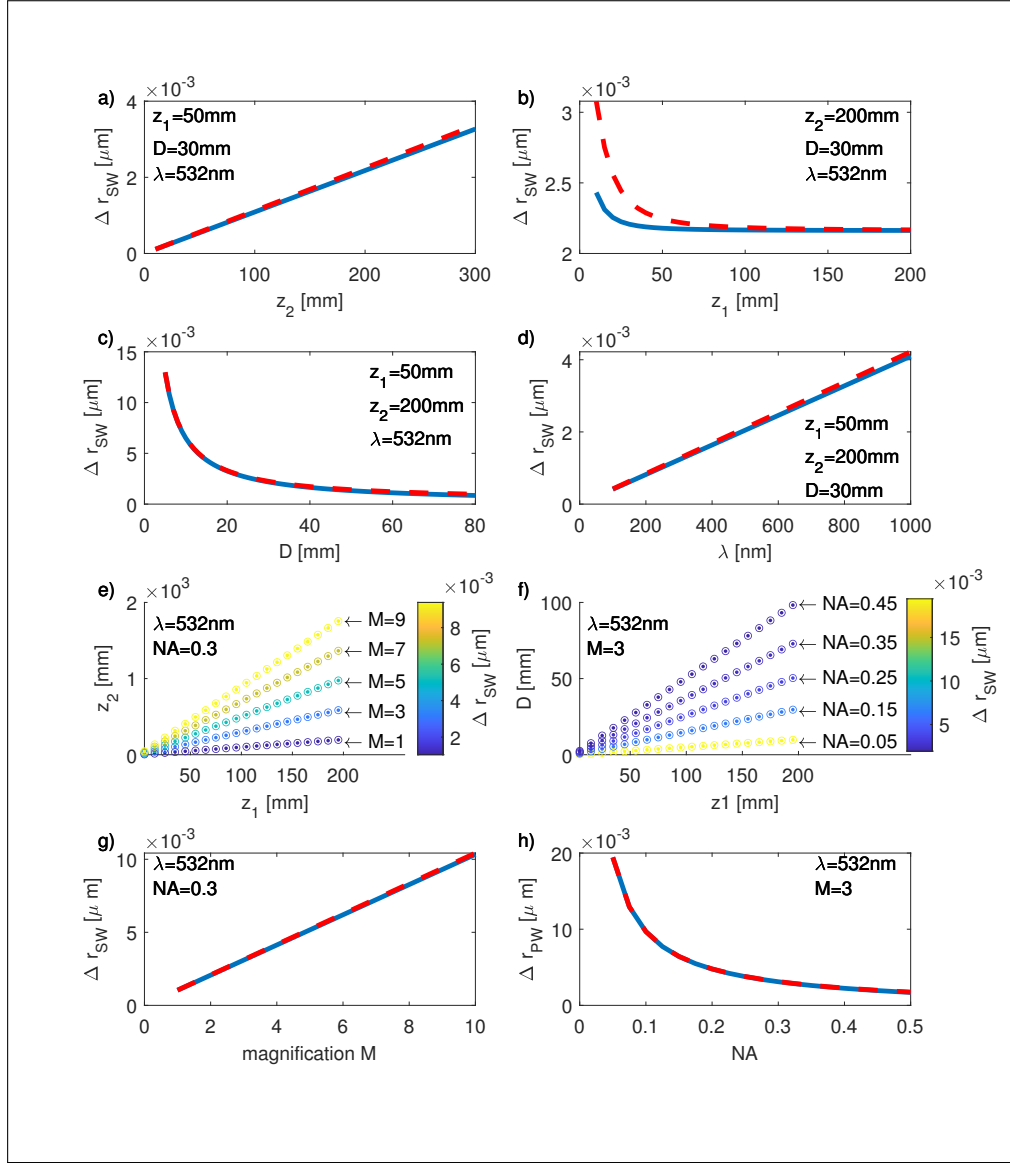


Fig. S1. Dependence of the speckle sizes in SPM on the parameters z_2 (a), z_1 (b), D (c) and λ (d). e) and g) show the speckle size in dependence on the magnification M for fixed NA, f) and h) show the speckle size in dependence on the NA for fixed M . Red dashed lines respectively unfilled circles show the results obtained with Eq. (S8), blue lines and dots show results obtained by numerically evaluating Eq. (S5).